Pancreatology 19 (2019) 331–339

Contents lists available at ScienceDirect

Pancreatology

journal homepage: www.elsevier.com/locate/pan

Prognostic evaluation of pancreatic ductal adenocarcinoma: Associations between molecular biomarkers and CT imaging findings

Yoshifumi Noda [a, *], Satoshi Goshima [a], Yusuke Tsuji [b], Hiroyuki Tomita [c], Akira Hara [c], Masaya Kawaguchi [a], Hiroshi Kawada [a], Nobuyuki Kawai [a], Yukichi Tanahashi [a], Masayuki Matsuo [a]

[a] Department of Radiology, Gifu University, 1-1 Yanagido, Gifu 501-1194, Japan
[b] Department of Radiology, Kyoto Prefectural University of Medicine, Kyoto, Japan
[c] Department of Tumor Pathology, Gifu University, Gifu, Japan

ARTICLE INFO

Article history:
Received 29 October 2018
Received in revised form
17 January 2019
Accepted 20 January 2019
Available online 24 January 2019

Keywords:
Pancreatic ductal carcinomas
Multidetector computed tomography
Epithelial-mesenchymal transition

ABSTRACT

Objectives: To investigate association between molecular biomarkers and computed tomography (CT) imaging findings in patients with pancreatic ductal adenocarcinoma (PDAC).
Methods: Fifty-three consecutive patients with PDAC (34 men and 19 women; mean age, 70.6 ± 8.1 years; range, 56–86 years) who underwent dynamic contrast-enhanced CT prior to pancreatectomy were included. The Ki-67 index and expressions of E-cadherin, Vimentin, and TWIST were immunohistochemically evaluated. Qualitative image analysis and histogram analysis of CT numbers were conducted. Clinical and molecular biomarkers were tested as possible prognostic factors for overall survival (OS) using Kaplan–Meier method and Cox proportional hazards regression. In addition, associations between CT imaging findings and significant molecular biomarkers were investigated.
Results: The TNM stage ($P = 0.018$) and E-cadherin expression status ($P = 0.018$) were independently associated with OS. E-cadherin-negative PDACs had a worse prognosis than E-cadherin-positive PDACs (hazard ratio: 2.21). Irregular tumor margin was observed more frequently in E-cadherin-negative PDACs (54.7%) than in E-cadherin-positive PDACs (45.3%) ($P = 0.00054$). The kurtosis of CT number during the pancreatic parenchymal phase was significantly higher in E-cadherin-negative PDACs than in E-cadherin-positive PDACs ($P = 0.035$).
Conclusions: E-cadherin suppression was found to be a prognostic factor for OS in patients with PDAC, and irregular tumor margin and kurtosis of CT numbers during the pancreatic parenchymal phase could be indicators for E-cadherin suppression.
© 2019 IAP and EPC. Published by Elsevier B.V. All rights reserved.

Introduction

Pancreatic ductal adenocarcinoma (PDAC) is the fourth leading cause of cancer-related death in both males and females, and the estimated number of deaths from PDAC was 44,330 in the United States in 2018. The 5-year relative survival rate is approximately 8% in all stages [1]. Complete surgical resection is the only potentially curative treatment [2], and patient survival can be predicted on the basis of pathological characteristics of PDAC, such as degree of tumor differentiation; pathological T (pT), N (pN), and M (pM) stages; and positive resection margins [3]. However, a surgical specimen is required to evaluate these factors.

Several molecular biomarkers have been reported as predictive factors for overall survival (OS), including SMAD4, Ki-67 index, Vimentin, E-cadherin, SPARC, and TWIST [4]. Among these, Vimentin, E-cadherin, and TWIST are associated with epithelial-to-mesenchymal transition (EMT), which is a key step in primary tumor progression to metastasis [5]. EMT activates the development of tumor cells from an epithelial phenotype to a more motile mesenchymal phenotype [6]. It is relatively easy for EMT-positive tumor cells to enter the systemic circulation, metastasize to another site, and proliferate at the metastatic site [7]. Therefore, an increased number of EMT-positive tumor cells is associated with poor survival in patients with PDAC [8].

Dynamic contrast-enhanced CT is routinely performed for the

* Corresponding author.
E-mail address: noda1031@gifu-u.ac.jp (Y. Noda).

https://doi.org/10.1016/j.pan.2019.01.016
1424-3903/© 2019 IAP and EPC. Published by Elsevier B.V. All rights reserved.

preoperative evaluation of tumor extension and surgical resectability in patients with newly diagnosed PDAC. We speculated that preoperative CT demonstrates different imaging findings between EMT-positive and EMT-negative tumors and preoperatively predicts OS in patients with PDAC. To our knowledge, no published study has reported the relationship between CT imaging findings and molecular biomarkers associated with EMT. Thus, the purpose of our study was to determine prognostic factors in patients with PDAC and investigate association between molecular biomarkers and CT imaging findings.

Material and methods

Patients

This retrospective study was approved by our institutional review board, and written informed consent was waived. Between May 2008 and October 2017, 72 consecutive patients who underwent dynamic contrast-enhanced CT prior to pancreatectomy for PDAC and underwent histopathological diagnoses were enrolled. Nineteen of the 72 patients were excluded because of the status after neoadjuvant chemoradiation therapy ($n = 15$), R2 resection ($n = 3$), and the absence of visible tumor on preoperative CT images ($n = 1$). Thus, the remaining 53 patients (mean age, 70.6 ± 8.1 years; range, 56–86 years), including 34 men (mean age, 70.4 ± 7.7 years; range, 56–86 years) and 19 women (mean age, 71.4 ± 9.1 years; range, 56–86 years), comprised the study population.

All patients underwent endoscopic ultrasound-guided fine-needle aspiration biopsy for histopathological diagnosis prior to pancreatectomy. The interval between preoperative contrast-enhanced CT and pancreatectomy ranged from 5 to 79 days, with a median of 26 days. The breakdown of interval was 1–30 days ($n = 29$), 31–60 days ($n = 20$), and 61–79 days ($n = 4$). PDACs were located in the pancreatic head ($n = 37$), body ($n = 7$), and tail ($n = 9$). Thirty-seven patients underwent pancreaticoduodenectomy with pancreaticojejunostomy reconstruction, and 16 underwent distal pancreatectomy. A total of 53 lesions in 53 patients were histopathologically diagnosed as PDAC. The hospital information system was used to obtain patient information including age; sex; plasmatic carcinoembryonic antigen (CEA) and carbohydrate antigen (CA) 19-9 levels; pT, pN, and pM stages; TNM stage; tumor differentiation; and residual tumor (R) classification [9].

Adjuvant therapy included none ($n = 12$), gemcitabine (GEM) only ($n = 19$), S-1 (tegafur, gimeracil, and oteracil potassium) only ($n = 18$), GEM plus S-1 ($n = 1$), and S-1 plus radiation therapy ($n = 3$).

Contrast-enhanced CT technique

We used a 64- or 16-detector CT scanner (Discovery CT750 HD or LightSpeed Ultra 16; GE Healthcare, Milwaukee, WI, USA) with an automatic tube current modulation system. Thirty patients were scanned using the 64-detector CT scanner, and 23 were scanned using the 16-detector CT scanner. The tube current modulation system combined both z-axis and angular modulation of the X-ray tube current [in milliamperes (mA)] adjusted for the size and shape of individual patients monitored on a single scout scan, accounting for all three dimensions. On the basis of a single scout scan and a preset noise index [*i.e.*, 1 standard deviation (SD) of background noise], radiation exposure was adjusted during CT scanning to achieve an acceptable image noise level across the regions of interest (ROIs) by modulating the tube current as the scan encountered various anatomic thicknesses and asymmetries [10].

CT imaging parameters were as follows: tube voltage, 120 kV peak (kVp); noise index, 12.0 Hounsfield unit (HU) at 5-mm slice collimation; tube current, variable; detector configuration, 64 or 16 detectors with 0.625-mm section thickness; beam collimation, 40 or 10 mm; rotation time, 0.4, 0.5, or 0.6 s; pitch, 0.561:1 or 1.375:1; scan field-of-view, large body; and display field-of-view, 40 cm.

Contrast material containing 350 or 300 mg iodine per mL was intravenously injected at a fixed duration of 30 s. In all patients, 600 mg of iodine per kg of total body weight was administered. A circle with a diameter of 15–20 mm was placed as an ROI in the abdominal aorta at the level of the first lumbar vertebral body. Real-time fluoroscopic monitoring scans (120 kVp, 10 mA) were initiated 10 s after the injection of contrast material was started. The diagnostic CT scanning was started with an additional delay of 20 s for the pancreatic parenchymal, 50 s for the portal venous, and 160 s for the equilibrium phase after a threshold of a 100 HU increase in the abdominal aorta was detected by a bolus-tracking program (SmartPrep; GE Healthcare) [11,12].

Histopathological and immunohistochemical evaluation

All histopathological and immunohistochemical features of surgical specimens were newly evaluated by two experienced pathologists (A.H. and H.T., with 31 and 19 years of experience in tumor pathology, respectively) and a radiologist (Y.T., with 5 years of post-training experience in interpreting abdominal CT images) in consensus. Hematoxylin and eosin stained specimens were used for the histopathological evaluation of the TNM stage and R classification according to the Union for International Cancer Control [9]. Immunostaining was performed to grade the Ki-67 index and to evaluate E-cadherin, Vimentin, and TWIST expressions. Ki-67 immunoreactivity was evaluated according to the percentage of positive tumor nuclei. Grading criteria for the Ki-67 index were as follows: 0, 0%–15% of immunostained nuclei (low) and 1, >16% (high) [13]; those for E-cadherin expression were as follows: 0, 0%–50% (negative) and 1, >51% (positive) [7]; those for Vimentin expression were as follows: 0, 0%–10% (negative) and 1, >11% (positive) [13]; and those for TWIST expression were as follows: 0, 0% positive tumor cells (negative) and 1, >1% (positive) [7].

Qualitative image analysis

Two experienced radiologists (S.G. and H.K., with 18 and 9 years of post-training experience at interpreting abdominal CT images, respectively) with no specific knowledge of the patients' clinical course or surgical outcome independently assessed CT images and in consensus. They reviewed tumor characteristics and the presence or absence of direct invasion to adjacent structures in reference to transaxial, coronal, and sagittal images during the precontrast, pancreatic parenchymal, portal venous, and equilibrium phases. A junior abdominal radiologist first reviewed CT images and then senior abdominal radiologist reviewed CT images. For any different opinions, the senior abdominal radiologist's reading was basically accepted as the standard.

The radiologists evaluated tumor characteristics including homogeneity, margin, and lymph node enlargement. Tumor homogeneity was classified as either homogeneous or heterogeneous; heterogeneous tumor was defined as that with mixed density necrosis and/or hemorrhage [14]. Tumor margin was classified as smooth or irregular; irregular margin was defined as a tumor with >70% of spiculated and/or infiltrative involvement [14]. Lymph node enlargement was defined by a minor axis >10 mm and/or central necrosis [15]. The radiologists also analyzed the presence or absence of direct invasion to adjacent structures, including the common bile duct, duodenum, pancreatic serosa, retroperitoneum, portal vein, major regional artery, plexus of the nerve, and other

organs [16].

Quantitative image analysis

An experienced radiologist (N.K., with 6 years of post-training experience at interpreting abdominal CT images) with no specific knowledge of the patients' clinical course or surgical outcome reviewed the CT images. The radiologist measured the maximal diameters of the main pancreatic and common bile ducts and the anterior–posterior (AP) diameters of the pancreatic head, body, and tail. In addition, the radiologist measured CT number for PDAC on transaxial images during the precontrast, pancreatic parenchymal, portal venous, and equilibrium phases using commercially available digital imaging software and a Communications in Medicine viewer (ShadeQuest ViewR; Yokogawa Medical Solutions, Tokyo, Japan), which was programmed to perform histogram analyses. For each phase, the mean CT number (HU) was measured using a circular ROI cursor drawn on the images showing a maximum diameter of PDAC to encompass as much of the lesion as possible while avoiding artifacts and large vessels. A series of histogram parameters, including the mean; median; mode; standard deviation; variance; kurtosis; skewness; coefficient of variance; minimum; maximum; entropy; energy; and 10th, 25th, 50th, 75th, and 90th percentiles were calculated.

Statistical analysis

Statistical analyses were conducted using MedCalc Statistical Software for Windows (MedCalc Software version 18.5, Mariakerke, Belgium).

In the first step, Kaplan–Meier method and log-rank test were conducted for univariate analysis and Cox proportional hazard regression was conducted for multivariate analysis to evaluate prognostic factors for OS in patients with PDAC. Patients' age; sex; diameters of the main pancreatic and common bile ducts; AP diameters of the pancreatic head, body, and tail; tumor location; plasmatic CEA and CA 19-9 levels; pT, pN, and pM stages; TNM stage; tumor differentiation; R classification; adjuvant therapy, Ki-67 index; and E-cadherin, Vimentin, and TWIST expressions were included as prognostic factors in the analysis. Further, prognostic factors that were statistically significant ($P < 0.05$) in univariate analysis were reassessed in multivariate analysis.

In the second step, association between molecular biomarkers identified as prognostic factors for OS in the first step and CT imaging findings was evaluated. The Mann–Whitney *U* test and Fisher's test were conducted to evaluate differences in the patients' background factors, tumor characteristics, and qualitative and quantitative parameters between molecular biomarker-positive and molecular biomarker-negative PDACs. For quantitative parameters, the optimal cutoff value was determined based on the highest area under the receiver operating characteristic (ROC) curve (AUC) yielding the highest sensitivity and specificity to differentiate between molecular biomarker-positive and molecular biomarker-negative groups. $P < 0.05$ was considered statistically significant.

Results

Patient demographics and tumor characteristics

Patients' demographics and tumor characteristics are summarized in Table 1. For Kaplan–Meier method and log-rank test, patients were classified into two groups using median values of age (71.0 years); diameters of the main pancreatic (4.4 mm) and common bile (6.8 mm) ducts; and AP diameters of the pancreatic head (17.0 mm), body (12.0 mm), and tail (11.0 mm). Plasma CEA (5.0 ng/mL) and CA 19–9 (37.0 U/mL) cutoff values were based on our institutional standard.

Overall survival and prognostic factors

The median follow-up duration was 16.0 (range, 3–112) months. Median OS was 24.0 (range, 3–39) months, and five (9.4%) patients were alive at the last follow-up for data collection.

Table 2 demonstrates the results of univariate and multivariate analyses of prognostic factors for OS. Significant prognostic factors for OS in univariate analysis were location [hazard ratio (HR), 1.00 in the pancreatic head, 3.21 in the pancreatic body, and 0.84 in the

Table 1
Patient demographics and tumor characteristics.

Characteristics	
Age (year)	70.6 ± 8.1 (56–86)
Gender (male:female)	34:19
Diameter of MPD (mm)	5.5 ± 3.6 (1.6–17.4)
Diameter of CBD (mm)	8.0 ± 4.2 (1.9–16.4)
AP diameter of pancreatic head (mm)	17.7 ± 3.3 (10.4–25.7)
AP diameter of pancreatic body (mm)	12.3 ± 3.6 (5.1–25.0)
AP diameter of pancreatic tail (mm)	11.7 ± 3.3 (5.3–19.7)
Location (head/body/tail)	37/7/9
CEA (ng/mL)	4.9 ± 3.8 (0.6–16.7)
CA19-9 (U/mL)	366.0 ± 689.1 (0.1–3410.8)
pT stage (1/2/3/4)	5/6/41/1
pN stage (0/1)	26/27
pM stage (0/1)	53/0
TNM stage (IA/IB/IIA/IIB/III/IV)	5/4/16/26/1/1
Tumor differentiation (wel/mod/por)	16/34/3
R classification (0/1)	44/9
Adjuvant therapy (none/GEM/S-1/GEM + S-1/S-1+RT)	12/19/18/1/3
Ki 67	21.3 ± 9.9 (5.0–47.9)
E-cadherin (negative/positive)	29/24
Vimentin (negative/positive)	45/8
TWIST (negative/positive)	10/43

Note.– Data are means ± 1 standard deviation with ranges in parentheses.
MPD = main pancreatic duct. CBD = common bile duct. AP = anterior-posterior. CEA = carcinoembryonic antigen. CA19-9 = carbohydrate antigen 19–9. GEM = gemcitabine. S-1 = tegafur, gimeracil, and oteracil potassium. RT = radiation therapy.

Table 2
Univariate and multivariate analyses for prediction of overall survival.

Prognostic Factors	Univariate Analysis		Multivariate Analysis	
	Hazard Ratio	*P* value	Hazard Ratio	*P* value
Age		0.13		
≤71.0 years	1			
>71.0 years	1.64			
Gender		0.83		
Male	1			
Female	0.93			
Diameter of MPD		0.70		
≤4.4 mm	1			
>4.4 mm	1.14			
Diameter of CBD		0.98		
≤6.8 mm	1			
>6.8 mm	0.99			
AP diameter of pancreatic head		0.93		
≤17.0 mm	1			
>17.0 mm	1.03			
AP diameter of pancreatic body		0.23		
≤12.0 mm	1			
>12.0 mm	1.48			
AP diameter of pancreatic tail		0.37		
≤11.0 mm	1			
>11.0 mm	1.34			
Location		0.0086*	0.94	0.76
Head	1			
Body	3.21			
Tail	0.84			
CEA		0.82		
≤5 ng/mL	1			
>5 ng/mL	0.92			
CA19-9		0.18		
≤37 U/mL	1			
>37 U/mL	1.78			
pT stage		<0.0001*	0.24	0.067
1	1			
2	2.70			
3	4.63			
4	107.9			
pN stage		0.47		
0	1			
1	1.26			
TNM stage		<0.0001*		0.018*
IA	1		0.025	
IB	0.97		0.059	
IIA	5.63		0.20	
IIB	4.63		0.75	
III	107.9		0.77	
IV	–		0.003	
Tumor differentiation		0.22		
Well	1			
Moderate	1.79			
Poorly	2.29			
R classification		0.15		
R0	1			
R1	1.78			
Adjuvant therapy		0.17		
none	1			
GEM	1.44			
S-1	2.64			
GEM + S-1	0.91			
S-1+RT	0.71			
Ki 67		0.72		
Low	1			
High	1.14			
E-cadherin		0.017*	2.34	0.018*
Positive	1			
Negative	2.21			
Vimentin		0.79		
Negative	1			
Positive	1.13			
TWIST		0.99		
Negative	1			
Positive	1			

Note.– MPD = main pancreatic duct. CBD = common bile duct. AP = anterior-posterior. CEA = carcinoembryonic antigen. CA19-9 = carbohydrate antigen 19–9. GEM = gemcitabine. S-1 = tegafur, gimeracil, and oteracil potassium. RT = radiation therapy.
*$P < 0.05$, significant difference.

pancreatic tail; $P = 0.0086$], pT stage (HR, 1.00 in pT1, 2.70 in pT2, 4.63 in pT3, and 107.9 in pT4; $P < 0.0001$), TNM stage (HR, 1.00 in stage IA, 0.97 in stage IB, 5.63 in stage IIA, 4.63 in stage IIB, and 107.9 in stage III; $P < 0.0001$), and E-cadherin expression status (HR, 1.00 in positive and 2.21 in negative; $P = 0.017$). Among these prognostic factors, the TNM stage ($P = 0.018$) and E-cadherin expression status ($P = 0.018$) remained statistically significant in multivariate analysis.

Associations between background factors and E-cadherin expression status

Patients' demographics and tumor characteristics between E-cadherin-negative and E-cadherin-positive PDACs are summarized in Table 3. Among 53 PDACs, 29 (54.7%) were E-cadherin-negative and 24 (45.3%) were E-cadherin-positive (Fig. 1). Plasma CA 19-9 level was significantly higher in E-cadherin-negative PDACs than in E-cadherin-positive PDACs ($P = 0.047$). The proportion of pN1 was significantly greater in E-cadherin-negative PDACs than in E-cadherin-positive PDACs ($P = 0.028$). No significant difference was found in terms of other parameters between E-cadherin-negative and E-cadherin-positive PDACs ($P = 0.059–1.00$).

Associations between qualitative imaging features and E-cadherin expression status

Tumor characteristics and the presence or absence of direct invasion to adjacent structures between E-cadherin-negative and E-cadherin-positive PDACs are summarized in Table 4. The proportion of irregular tumor margin was significantly higher in E-cadherin-negative than in E-cadherin-positive PDACs ($P = 0.00054$) (Fig. 2). No significant difference was found for the other tumor characteristics between E-cadherin-negative and E-cadherin-positive PDACs ($P = 0.086–1.00$).

Table 3
Patient demographics and tumor characteristics between E-cadherin negative and positive pancreatic ductal adenocarcinomas.

	E-cadherin negative ($n = 29$)	E-cadherin positive ($n = 24$)	*P* value
Age (year)	70.3 ± 8.2 (56–86)	71.3 ± 8.3 (56–86)	0.57
Gender (male:female)	16:13	18:6	0.16
Diameter of MPD (mm)	5.99 ± 3.9 (2.0–17.4)	4.88 ± 3.1 (1.6–13.7)	0.24
Diameter of CBD (mm)	8.30 ± 4.3 (2.3–16.4)	7.56 ± 4.0 (1.9–16.2)	0.57
AP diameter of pancreatic head (mm)	17.9 ± 3.0 (10.4–23.3)	17.5 ± 3.6 (10.6–25.7)	0.56
AP diameter of pancreatic body (mm)	12.9 ± 3.8 (6.2–25.0)	11.7 ± 3.2 (5.1–18.4)	0.32
AP diameter of pancreatic tail (mm)	12.2 ± 3.3 (6.6–19.7)	11.1 ± 3.3 (5.3–18.8)	0.23
Location (head/body/tail)	19/5/5	18/2/4	0.70
CEA (ng/mL)	4.3 ± 3.5 (0.9–15.1)	5.6 ± 4.1 (0.6–16.7)	0.18
CA19-9 (U/mL)	504.1 ± 859.5 (0.1–3410.8)	199.3 ± 348.2 (0.4–1495.6)	0.047*
pT stage (1/2/3/4)	2/3/24/0	3/3/17/1	0.58
pN stage (0/1)	10/19	16/8	0.028*
pM stage (0/1)	29/0	24/0	1.00
TNM stage (IA/IB/IIA/IIB/III/IV)	2/1/7/18/0/1	3/3/9/8/1/0	0.22
Tumor differentiation (wel/mod/por)	6/20/3	10/14/0	0.18
R classification (0/1)	23/6	21/3	0.49
Adjuvant therapy (none/GEM/S-1/GEM + S-1/S-1+RT)	7/13/8/1/0	5/6/10/0/3	0.14
Ki 67 (low/high)	10/19	12/12	0.25
Vimentin (negative/positive)	22/7	23/1	0.059
TWIST (negative/positive)	8/21	2/22	0.091

Note.– Data are means ± 1 standard deviation with ranges in parentheses.
MPD = main pancreatic duct. CBD = common bile duct. AP = anterior-posterior. CEA = carcinoembryonic antigen. CA19-9 = carbohydrate antigen 19–9. GEM = gemcitabine. S-1 = tegafur, gimeracil, and oteracil potassium. RT = radiation therapy.
*$P < 0.05$, significant difference.

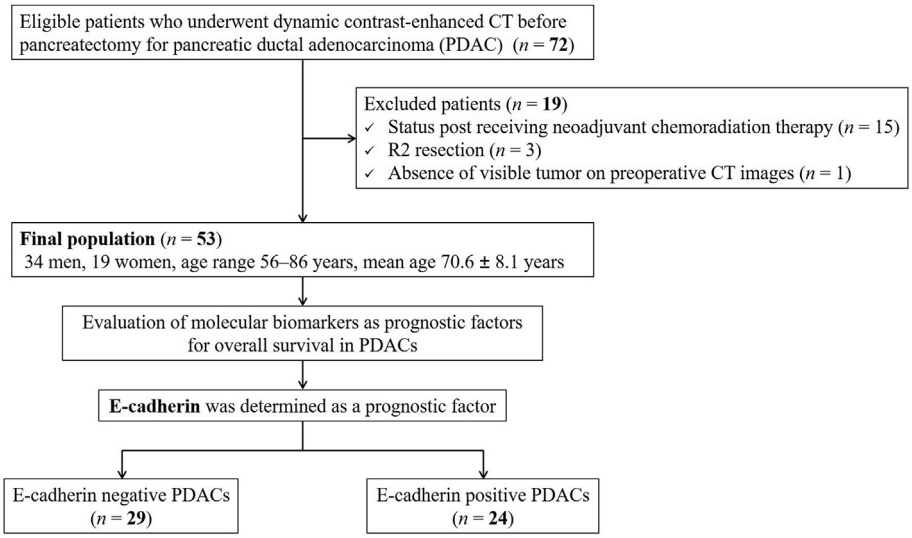

Fig. 1. Flow chart of included and excluded patients.

Table 4
Qualitative imaging features between E-cadherin negative and positive pancreatic ductal adenocarcinomas.

	E-cadherin negative ($n = 29$)	E-cadherin positive ($n = 24$)	P value
Tumor characteristics			
Homogeneity			0.77
Homogeneous	20	15	
Heterogeneous	9	9	
Margins			0.00054*
Smooth	5	16	
Irregular	24	8	
IPMN background			1.00
Absence	24	19	
Presence	5	5	
Lymph node enlargement			0.49
Absence	27	24	
Presence	2	0	
Metastasis			1.00
Absence	29	24	
Presence	0	0	
Tumor invasion			
Common bile duct			0.78
Absence	15	14	
Presence	14	10	
Duodenum			0.76
Absence	20	18	
Presence	9	6	
Pancreatic serosa			0.59
Absence	12	12	
Presence	17	12	
Retroperitoneum			1.00
Absence	12	10	
Presence	17	14	
Portal vein			1.00
Absence	22	19	
Presence	7	5	
Major regional artery			0.086
Absence	29	21	
Presence	0	3	
Plexus of the nerve			1.00
Absence	28	24	
Presence	1	0	
Other organs			0.49
Absence	27	24	
Presence	2	0	

*$P < 0.05$, significant difference.

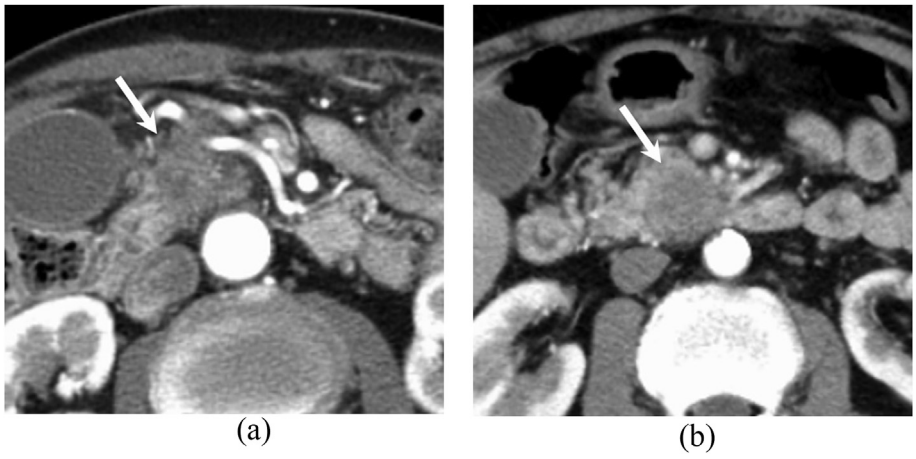

Fig. 2. (a) A 65-year-old man with pancreatic ductal adenocarcinoma of the head (arrow). The tumor margin is irregular, and this tumor was diagnosed as E-cadherin-negative pancreatic ductal adenocarcinoma (PDAC). The survival duration was 24 months. **(b)** A 69-year-old man with PDAC of the head (arrow). The tumor margin is well defined, and this tumor was diagnosed as E-cadherin-positive PDAC. This patient was alive at 33-month follow-up for data collection.

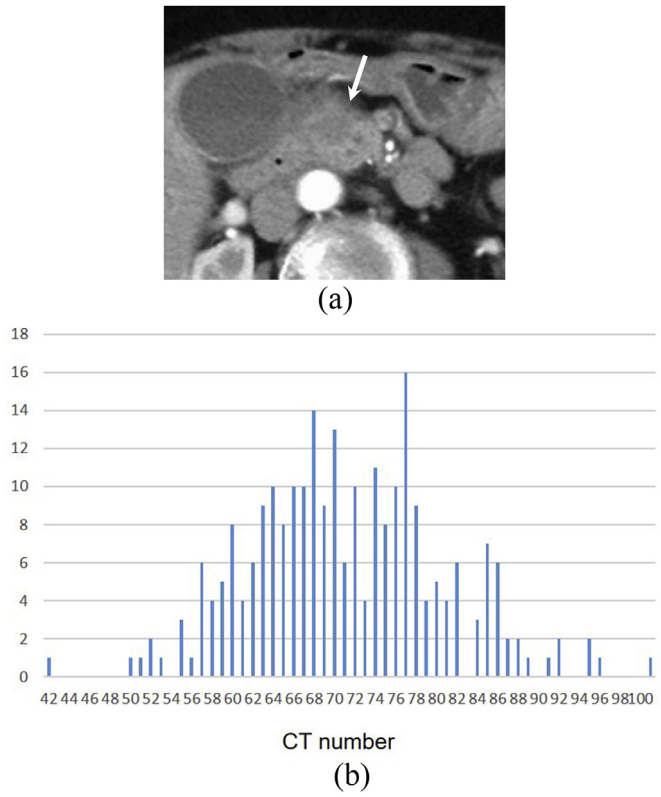

Fig. 3. **(a)** A 69-year-old man with PDAC of the head (arrow). **(b)** Histogram analysis showed that the kurtosis of CT number during the pancreatic parenchymal phase was 3.12, which was greater than the cutoff value of 2.55, and this tumor was diagnosed as E-cadherin-negative PDAC. The survival duration was 15 months.

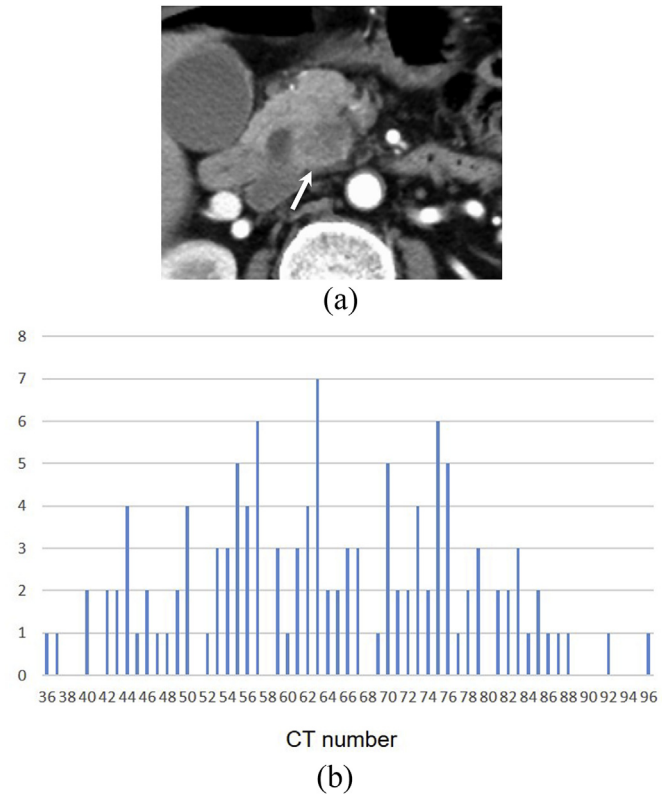

Fig. 4. **(a)** A 70-year-old man with pancreatic ductal adenocarcinoma of the head (arrow). **(b)** Histogram analysis showed that the kurtosis of CT number during the pancreatic parenchymal phase was 2.25, which was lower than the cutoff value of 2.55, and this tumor was diagnosed as E-cadherin-positive PDAC. The survival duration was 28 months.

Associations between quantitative imaging features and E-cadherin expression status

The kurtosis of CT number during the pancreatic parenchymal phase was significantly higher in E-cadherin-negative PDACs than in E-cadherin-positive PDACs (mean value, 3.02 ± 0.44; range, 2.23–4.08 vs. mean value, 2.72 ± 0.56; range, 1.94–4.08; $P = 0.035$) (Figs. 3–5). No significant difference was found in other histogram parameters between E-cadherin-negative PDACs and E-cadherin-positive PDACs ($P = 0.061$–0.99). Based on ROC analysis, the cutoff value of the kurtosis of CT number during the pancreatic parenchymal phase for differentiating E-cadherin-negative and E-cadherin-positive PDACs was 2.55. Sensitivity, specificity, and AUC for differentiating between E-cadherin-negative and E-cadherin-positive PDACs were 89.7%, 50.0%, and 0.67, respectively, when using this cutoff value (Fig. 6).

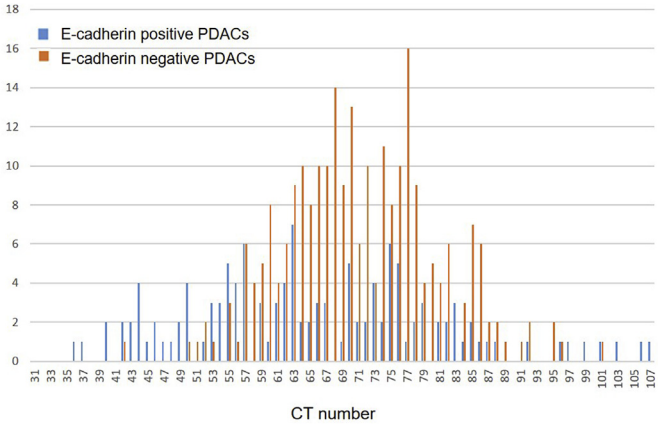

Fig. 5. Histogram analysis showed that the kurtosis of CT number during the pancreatic parenchymal phase of E-cadherin-positive and E-cadherin-negative PDACs as blue and orange bars, respectively. The histogram of E-cadherin-negative PDACs showed sharper peak compared with E-cadherin-positive PDACs.

Overall survival in patients with E-cadherin negative and positive PDACs

The median OS rate was significantly lower in patients with E-cadherin-negative PDACs than in those with E-cadherin-positive PDACs (72.2% vs. 83.1% at 1 year; 67.1% vs. 35.3% at 2 years; and 44.8% vs. 8.3% at 3 years, respectively; $P = 0.017$ by log-rank test) (Fig. 7).

Discussion

Our study demonstrated that among clinical and pathological prognostic factors, TNM stage and E-cadherin expression status were significantly associated with OS in patients with PDACs. Thus, although it may be reasonable that TNM stage was determined as a prognostic factor for OS in PDAC, E-cadherin expression status in PDAC was also determined as a prognostic factor. A partial or complete loss of E-cadherin expression was significantly associated with tumor metastases including lymph nodes and/or poor survival in patients with PDAC [17,18]. Lymph node metastasis was more frequently observed and plasma CA 19-9 level was significantly

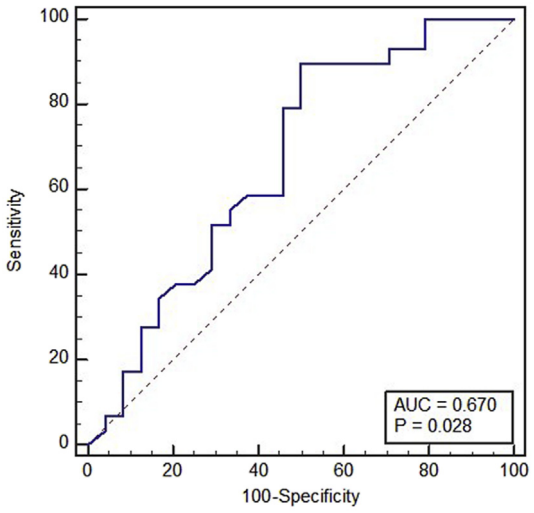

Fig. 6. Receiver operating characteristic (ROC) curve for differentiating between E-cadherin-negative and E-cadherin-positive PDACs. Area under the ROC curve in the kurtosis of CT number during the pancreatic parenchymal phase was 0.67.

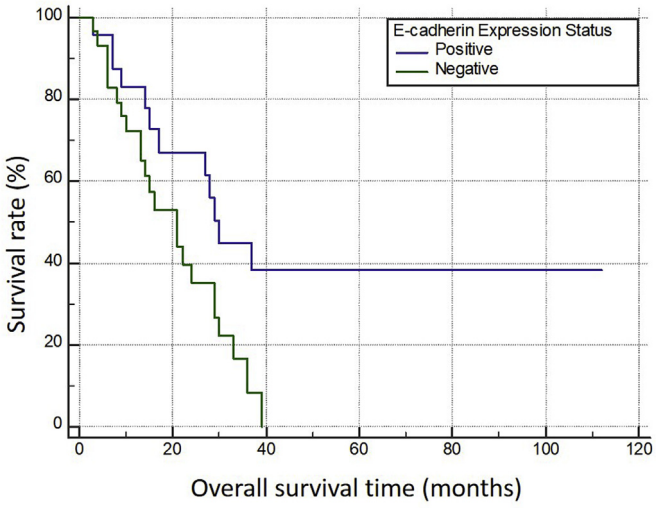

Fig. 7. Kaplan–Meier overall survival curves for E-cadherin-positive versus E-cadherin-negative PDACs. E-cadherin negative PDACs had a significantly worse overall survival rate than E-cadherin-positive PDACs ($P = 0.017$).

higher in E-cadherin-negative PDACs than in E-cadherin-positive PDACs in the present study. E-cadherin, a cell adhesion molecule, is an essential protein associated with EMT. It was assumed that because tumor cell adhesion is disassembled with reduced E-cadherin expression [19], the tumor obtains a higher invasive capacity.

In addition, among the CT findings, irregular tumor margin in qualitative image analysis and the kurtosis of CT number during the pancreatic parenchymal phase in quantitative image analysis were significantly associated with the E-cadherin expression status. In the present study, irregular tumor margin was more frequently observed in E-cadherin-negative PDACs, which may reflect the more invasive capacity of E-cadherin-negative PDACs. E-cadherin-negative PDACs get a more motile activity, therefore, we believed that tumor margins of E-cadherin-negative PDACs tended to be more spiculated and/or infiltrative than those of E-cadherin-positive PDACs. According to a previous study, well-defined tumor margin was associated with the expression of DPC4, which is a tumor suppressor gene, and represented a less infiltrative disease behavior [14].

Tumor aggressiveness, angiogenesis, and distant metastasis in several cancers are associated with hypoxia. Generally, as the tumor grows, the central portion of the cancer becomes hypoxic, hypovascular, and necrotic [20]. In this study, the kurtosis of CT number during the pancreatic parenchymal phase in PDACs was significantly higher in E-cadherin-negative PDACs than in E-cadherin-positive PDACs, whereas the mean CT number during the pancreatic parenchymal phase was comparable between the two tumor groups. Kurtosis represents the peaks and widths in the distribution of metrics. A higher kurtosis indicates a relatively sharper peak with wider tails. Related hypoxia factors play a crucial role in EMT, and a previous report showed that hypoxia-inducible factor-2α promotes EMT in PDAC by regulating TWIST2 binding to the promotor of E-cadherin [21]. Our results may reflect the heterogeneity of E-cadherin-negative PDACs, including the mixture of hypovascular and necrotic components, compared with that of E-cadherin-positive PDACs.

Our study had several limitations. First, it was a retrospective study with a relatively small sample size, which may have caused a selection bias. Second, two CT scanners were used and one was relatively outdated CT scanner because of the retrospective study design with a relatively long time period. Third, we did not evaluate whether the E-cadherin expression status is related to response to the post-surgical treatment. A previous report demonstrated that PDADs with high kurtosis of iodine concentration at pancreatic parenchymal phase in dual-energy CT were resistant to chemotherapy compared with those with low kurtosis [22]. Therefore, we believed that E-cadherin-negative PDACs tend to be resistant to post-surgical treatment in an indirect manner. Finally, limited molecular biomarkers were evaluated. Several molecular biomarkers are associated with the prognosis of PDACs, including DPC4, SPARC, BCL2, and BRCA2 [4]. Despite these limitations, some CT imaging findings were linked to molecular biomarkers associated with OS in patients with PDAC in this study. Further clinical studies with larger sample sizes are prospectively needed to validate our results.

In conclusion, E-cadherin suppression was a prognostic factor associated with OS in patients with PDAC, and irregular tumor margin and the kurtosis of CT number during the pancreatic parenchymal phase could be indicators of E-cadherin suppression. Preoperative assessment of E-cadherin expression status is beneficial for personalized medicine and improvement of prognosis in patients with PDAC.

Conflicts of interest

Author disclosure of potential conflict of interest. No relevant conflicts of interest to disclose.

References

[1] Siegel RL, Miller KD, Jemal A. Cancer statistics. CA A Cancer J Clin 2018;68:7–30.
[2] Campbell F, Smith RA, Whelan P, Sutton R, Raraty M, Neoptolemos JP, et al. Classification of r1 resections for pancreatic cancer: the prognostic relevance of tumour involvement within 1 mm of a resection margin. Histopathology 2009;55:277–83.
[3] Hidalgo M. Pancreatic cancer. N Engl J Med 2010;362:1605–17.
[4] Martinez-Useros J, Garcia-Foncillas J. Can molecular biomarkers change the paradigm of pancreatic cancer prognosis? BioMed Res Int 2016;2016:4873089.
[5] Boyer B, Valles AM, Edme N. Induction and regulation of epithelial-mesenchymal transitions. Biochem Pharmacol 2000;60:1091–9.
[6] Huber MA, Kraut N, Beug H. Molecular requirements for epithelial-mesenchymal transition during tumor progression. Curr Opin Cell Biol 2005;17:548–58.
[7] Hotz B, Arndt M, Dullat S, Bhargava S, Buhr HJ, Hotz HG. Epithelial to mesenchymal transition: expression of the regulators snail, slug, and twist in

pancreatic cancer. Clin Canc Res : an official journal of the American Association for Cancer Research 2007;13:4769–76.
[8] Masugi Y, Yamazaki K, Hibi T, Aiura K, Kitagawa Y, Sakamoto M. Solitary cell infiltration is a novel indicator of poor prognosis and epithelial-mesenchymal transition in pancreatic cancer. Hum Pathol 2010;41:1061–8.
[9] Wittekind C, Compton CC, Greene FL, Sobin LH. Tnm residual tumor classification revisited. Cancer 2002;94:2511–6.
[10] Kalra MK, Maher MM, Toth TL, Schmidt B, Westerman BL, Morgan HT, et al. Techniques and applications of automatic tube current modulation for ct. Radiology 2004;233:649–57.
[11] Goshima S, Kanematsu M, Kondo H, Yokoyama R, Miyoshi T, Kato H, et al. Pancreas: optimal scan delay for contrast-enhanced multi-detector row ct. Radiology 2006;241:167–74.
[12] Kondo H, Kanematsu M, Goshima S, Miyoshi T, Shiratori Y, Onozuka M, et al. Mdct of the pancreas: optimizing scanning delay with a bolus-tracking technique for pancreatic, peripancreatic vascular, and hepatic contrast enhancement. AJR American journal of roentgenology 2007;188:751–6.
[13] Myoteri D, Dellaportas D, Lykoudis PM, Apostolopoulos A, Marinis A, Zizi-Sermpetzoglou A. Prognostic evaluation of vimentin expression in correlation with ki67 and cd44 in surgically resected pancreatic ductal adenocarcinoma. Gastroenterol Res Pract 2017;2017:9207616.
[14] Choi SH, Kim HJ, Kim KW, An S, Hong SM, Kim SC, et al. Dpc4 gene expression in primary pancreatic ductal adenocarcinoma: relationship with ct characteristics. Br J Radiol 2017;90:20160403.
[15] Al-Hawary MM, Francis IR, Chari ST, Fishman EK, Hough DM, Lu DS, et al. Pancreatic ductal adenocarcinoma radiology reporting template: consensus statement of the society of abdominal radiology and the american pancreatic association. Radiology 2014;270:248–60.
[16] Noda Y, Goshima S, Kawada H, Kawai N, Miyoshi T, Matsuo M, et al. Modified national comprehensive cancer network criteria for assessing resectability of pancreatic ductal adenocarcinoma. AJR American journal of roentgenology 2018;210:1252–8.
[17] Hong SM, Li A, Olino K, Wolfgang CL, Herman JM, Schulick RD, et al. Loss of e-cadherin expression and outcome among patients with resectable pancreatic adenocarcinomas. Mod Pathol : an official journal of the United States and Canadian Academy of Pathology 2011;24:1237–47. Inc.
[18] Guo S, Xu J, Xue R, Liu Y, Yu H. Overexpression of aib1 correlates inversely with e-cadherin expression in pancreatic adenocarcinoma and may promote lymph node metastasis. Int J Clin Oncol 2014;19:319–24.
[19] Lamouille S, Xu J, Derynck R. Molecular mechanisms of epithelial-mesenchymal transition. Nat Rev Mol Cell Biol 2014;15:178–96.
[20] Miles KA. Tumour angiogenesis and its relation to contrast enhancement on computed tomography: a review. Eur J Radiol 1999;30:198–205.
[21] Yang J, Zhang X, Zhang Y, Zhu D, Zhang L, Li Y, et al. Hif-2alpha promotes epithelial-mesenchymal transition through regulating twist2 binding to the promoter of e-cadherin in pancreatic cancer. J Exp Clin Canc Res : CR 2016;35:26.
[22] Noda Y, Goshima S, Miyoshi T, Kawada H, Kawai N, Tanahashi Y, et al. Assessing chemotherapeutic response in pancreatic ductal adenocarcinoma: histogram analysis of iodine concentration and ct number in single-source dual-energy ct. AJR American journal of roentgenology 2018;211:1221–6.